Supplemental material for "Dynamic structure factors of Cu, Ag, and Au: A comparative study from first principles"

A. Alkauskas, S. D. Schneider, C. Hébert, S. Sagmeister, and C. Draxl

I. DIELECTRIC FUNCTIONS OF Cu, Ag, AND Au FOR SMALL ENERGIES

In this Section, we present a unifying analysis of the loss functions for all Cu, Ag, and Au at energies below 10 eV. We provide an of the reasons why the plasmon forms in Ag, but is absent in the two other metals. This analysis complements that of Cazalilla *et al.* [1] and is based on the properties of coupled classical Drude-Lindhard oscillators [2]. The same classical model explains why the plasmon in Ag, when calculated using semilocal density functionals (the local density approximation, LDA, and various versions of GGA), has a much lower energy, is much broader, and less intense than in experiment.

In Fig. 1, GGA band structures and total densities of states (DOS) are presented. The occupied part of the DOS of all three metals is characterized by a sharp feature 3-4 eV wide that originates from d bands, superimposed on a smooth background DOS originating from sp bands [3]. Since in the main article our emphasis is on excitations with final states high above the Fermi level, it is important that the band structure at those energies is accurately described. A large basis set for electronic wavefunctions and, more importantly, an all-electron approach is therefore essential. We note two important conclusions about the unoccupied part of the DOS in these three metals: (i) Above the Fermi level the DOS is approximately given by that of the free electron gas (in atomic units) $D(E) = \sqrt{2m^3(E - E_0)}/\pi^2 n$, where E_0 is the bottom of the sp band, n is valence electron density excluding d electrons, and m is the effective electron mass (best fits are obtained with $m = 1$). However, even for the highest energies studied, the DOS shows small oscillations due to the underlying atomic structure and does not attain a smooth behavior, which is characteristic of the free electron gas. The most pronounced oscillations in the DOS are indeed physical and directly translate into features in the loss function that are measured experimentally, as discussed in the main article. This conclusion is also in full agreement with Bremsstrahlung isochromate spectroscopy (BIS) measurements of Speier *et al.* [4]. In passing, we note that this aspect is also relevant in interpreting photo-emission experiments.

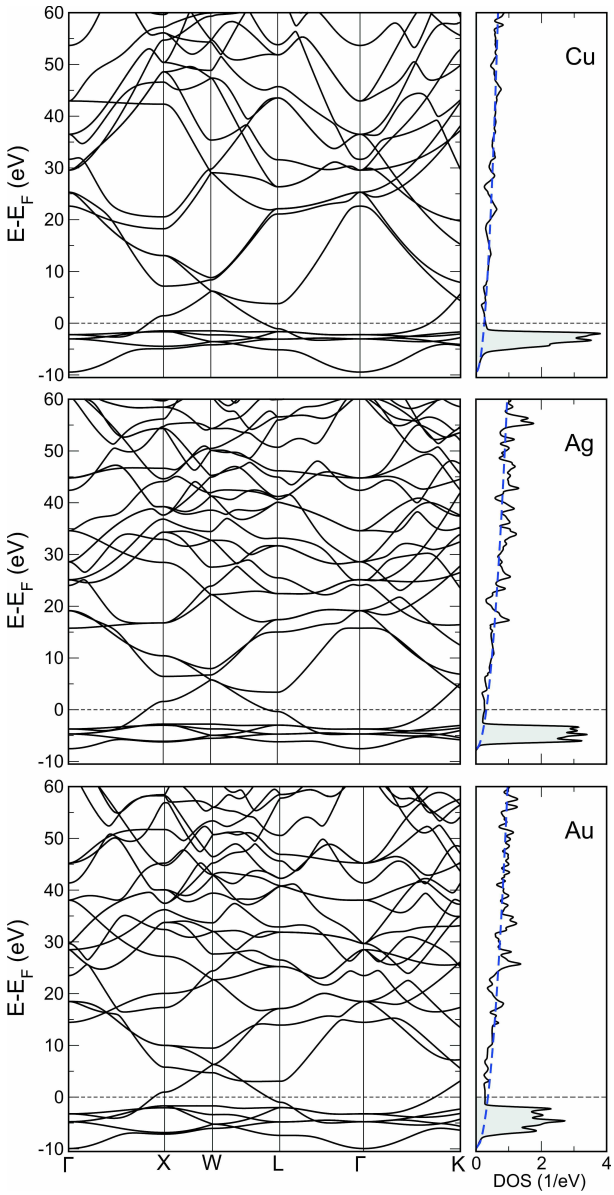

FIG. 1: (Color online) Calculated band structures (left) and density of states (right) of Cu, Ag, and Au in the energy range −10-60 eV with respect to the Fermi level. Dashed lines represent the density of states of the free-electron gas, $D(E) = \sqrt{2m^3(E - E_0)}/\pi^2 n$, E_0 being the bottom of the *sp* band, m the electron mass, and $n = 1/(4a^3)$ valence electron density (without d electrons), a being the lattice constant.

During the photo-emission process, electrons are kicked out from the sample by incoming photons, thus they are often described as plane waves, even for moderate kinetic energies. The results in Fig. 1 show that for d metals such simplified behavior is not achieved for energies < 60 eV. (ii) Due to a smaller lattice constant of Cu (3.50 Å) in comparison to that

of Ag (4.09 Å) and Au (4.08 Å), electronic bands are more dispersive in Cu. Consequently, the total DOS of Cu is somewhat less structured.

The most interesting aspect of loss functions for small energies (< 10 eV) is the fact that a well-defined low-energy plasmon forms in Ag (at 3.8 eV), but is absent in other metals. As already discussed by Ehrenreich and Philipp [3, 5], it results from the interaction of collective oscillations of electrons in the *sp* band and the onset of strong optical absorption from 4*d* states. The latter significantly modifies the width and the energy of the plasmon peak. In the absence of such coupling, collective oscillations would occur at the frequency of the Drude plasmon, in Ag $\hbar\omega_{\mathrm{p}} \approx 9.7$ eV. (This value is derived from our calculations, but is very close to that obtained before [3].) Alternatively, the reduction of plasmon frequency in Ag could be thought of as a screening effect by the 4*d* electrons, i.e., $\Omega \approx \omega_{\mathrm{p}}/\sqrt{\varepsilon_{\mathrm{d}}}$ [6]. However, such reasoning cannot explain the absence of a similar excitation in Cu and Au.

Cazalilla and coworkers provided a fundamental argument explaining these features [1]. In short, the interaction of the Drude plasmon with interband excitations can be understood such as interband excitations act as a self-energy for the plasmon. A low-energy plasmon can thus occur if the real part of the dielectric function vanishes for a certain energy. This scenario is more likely if the onset of interband transitions appears at higher energies and (somewhat less important) if the oscillator strength of these transitions is larger. It was found that this happens only in Ag [1].

One can also see how the position of the *d* states influences the actual energy of the plasmon peak by using a phenomenological model. While this model is too simplistic to be applicable to real materials, it nevertheless captures the most essential physics of noble metals and complements the analysis of Refs. [1, 3, 5–7]. Let us consider a system in which Drude-type free electrons with plasma frequency ω_{p} coexist with a bound oscillator of frequency ω_1 [2]. This frequency corresponds to a strong optical absorption band which, in our case, is the onset of transitions from *d* states to the states above the Fermi level. If damping terms are small, the dielectric function is

$$\varepsilon(\omega) = 1 - \frac{\omega_{\mathrm{p}}^2}{\omega^2} + \frac{\omega_{\mathrm{p}}^2 f_1}{\omega_1^2 - \omega^2} \tag{1}$$

with f_1 being the oscillator strength for bound electrons.

Collective oscillations of the system occur where $\varepsilon(\omega) = 0$. For noble metals $\omega_{\mathrm{p}} \gg \omega_1$, and the two frequencies at which Eq. (1) becomes zero are approximately $\omega_1 \left[1/(1+f_1)\right]^{1/2}$ and

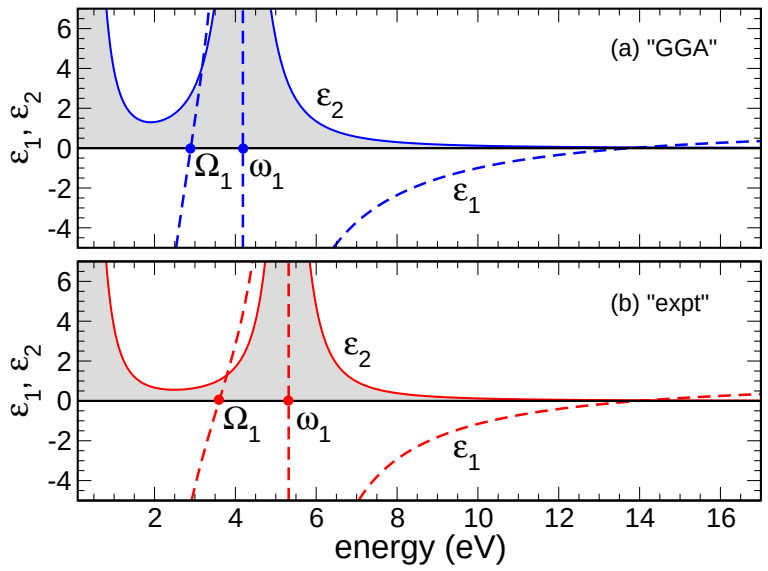

FIG. 2: Real part ε_1 (dashed line) and imaginary part ε_2 (full line) of the dielectric function for a system consisting of free Drude electrons and a bound oscillator with frequency ω_1. Compared to (b), ω_1 is smaller in (a), and the corresponding peak width is slightly broader. These two factors result in a pronounced plasmon excitation in (b) while the plasmon is severely damped in (a).

$\omega_p\,(1+f_1)^{1/2}$, only the first of which is relevant for our purposes. The best agreement for Ag is obtained for $f_1 = 1$, which we will assume here for qualitative considerations. Thus, the lowest collective oscillation in such system occurs at frequency $\Omega_1 \approx \omega_1/\sqrt{2}$. Whether the plasmon excitation actually develops or not depends on the imaginary part of the dielectric function at this frequency. If ε_2 is small, the plasmon can exist, while if ε_2 is large, the plasmon is severly damped.

Thus, in reality, damping terms must be included. They smoothen the function ε_1, and give a finite width to optical excitations seen in ε_2. Model dielectric functions are plotted in Fig. 2 for two different cases (for graphical purposes the damping terms are included only in ε_2). Say, ω_1 is underestimated by a certain theory which tries to model the real situation (Fig. 2(a)). As a result, Ω_1 will also be underestimated since $\Omega_1 \approx \omega_1/\sqrt{2}$. More importantly, this implies that Ω_1 is closer to ω_1 as $\omega_1 - \Omega_1 \approx \omega_1(1-1/\sqrt{2})$ (Fig. 2(a)). Since ε_2 peaks at $\omega = \omega_1$, the value of $\varepsilon_2(\Omega_1)$ will be larger (or much larger) in this approximation compared to reality. As a result, the plasmon excitation will be severely damped. Increasing the value of ω_1 (Fig. 2(b)) also increases the distance between Ω_1 and ω_1, and thus decreases the value of ε_2 at $\omega = \Omega_1$. Consequently, the plasmon peak becomes more pronounced. If,

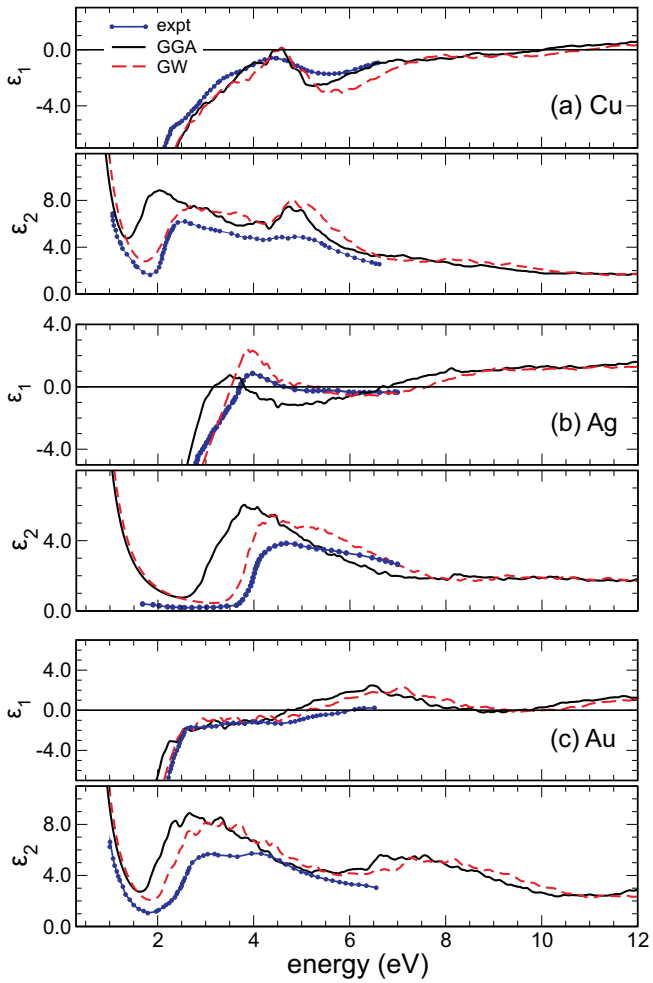

FIG. 3: (Color online) Calculated and measured (blue dots) dielectric functions for Cu, Ag, and Au in the energy range up to 12 eV. The calculations are performed using either the GGA band structure (black solid lines) or approximate *GW* corrections on top (red dashed lines).

in addition, the width of the peak in ε_2 around ω_1 was narrower in the improved theory (as happens in the case of Ag due to the reduced width of Ag $4d$ states), this facilitates the formation of the plasmon excitation further.

As can be seen from this simple model, it is very important to accurately represent the onset of optical transitions (ω_1 above) in order to have a reliable description of the plasmon. This conclusion is in full agreement with the analyses of Refs. [1, 3, 5–8]. In Cu, Ag, and Au this onset depends on the position of d states that has to be described correctly. It is well known that GGA functionals somewhat fail in this respect. This happens due to remaining self-interaction errors and (less importantly) many-body effects. To partially

cure these shortcomings, we have applied approximate GW corrections when calculating the non-interacting density response functions χ^0. We have used the GW results of Yu et al. [9] for Cu, Marini *et al.* [7] for Ag, and Rangel *et al.* [10] for Au. The corrections are functions only of energy. In case of Ag, for example, this approach is an approximation of that used in Ref. [7]. The calculated dielectric functions of all three metals are compared with each other and with available experimental results in Fig. 3. The corresponding loss functions are presented in Fig. 4.

Below, we give a brief discussion of the main features in dielectric and loss functions based on the phenomenological theory introduced above.

Copper. In comparison with local and semilocal functionals, GW pushes Cu $3d$ states down by about 0.8 eV. [9] As a result, the onset of the corresponding peak in ε_2 occurs at larger energies (Fig. 3(a)), in agreement with experiment. These corrections are substantial to recover a simulated reddish color of Cu (Fig. 5). However, $3d$ states are relatively shallow in Cu, and ε_1 does not become zero for small energies. That means that the low-energy plasmon excitation does not develop in Cu. Instead, a small broad peak (peak (1) in Fig. 4(a) and Fig. 1(a) of the main paper) appears. However, ε_1 vanishes at about 10 eV. This results in a wide peak in the loss function (peak (2) in Figs. 4 and 1(a) of the main paper), which should thus also be considered as a plasmon-type excitation. A simple classical model discussed above would yield a position of this second peak at about $\hbar\Omega_2 \approx \sqrt{2}\hbar\omega_\mathrm{p} \approx 14$ eV (using the parameters for Cu). This means that a simple model is unable to explain the actual position of this higher-lying peak, that results from the interaction of free electron in the *sp* band and the entire optical absorption band.

Silver. Silver is the only case in which a well-defined low-energy plasmon develops, as discussed above. This happens because Ag $4d$ states are deeper than the d states in the two other metals. Dielectric and loss functions of silver are thus most sensitive to details of the band structure, as seen in Figs. 3(b) and 4(b). Indeed, the absorption onset from Ag $4d$ states to states above the Fermi level, as seen from ε_2, is found by about 0.8 eV too low in energy in GGA. Because of an overestimated absorption in the blue range, this results in a dirty green color predicted by GGA (Fig. 5). The center of the first peak in ε_2 occurs at about 4.2 eV in GGA, and the model above would predict that ε_1 vanishes at $4.2/\sqrt{2} \approx 3.0$ eV, which is not far from the actual value of 3.2 eV. The plasmon excitation peaks at 3.0 eV, while the experimental plasmon energy is 3.8 eV. Due to the rather high value of ε_2 the

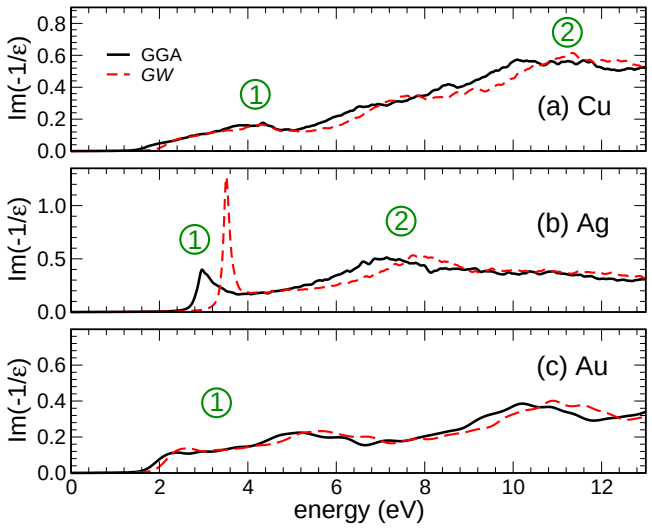

FIG. 4: Impact of exchange-correlation effects in the band structure on the loss functions of Cu, Ag, and Au: Solid lines obtained from GGA band structure and dashed lines from *GW* bands.

peak is much broader than the experimental one.

GW corrections shift Ag 4*d* states down by about 1.0 eV, and thus the center of the maximum in ε_2 shifts to about 5.0 eV, making silver appear gray (Fig. 5). According to the phenomenological model, ε_1 should vanish at about $5.0/\sqrt{2} \approx 3.5$ eV. The plasmon peak indeed develops at about 3.55 eV, in much better agreement with experiment. Moreover, the peak becomes much more narrow and well defined.

As seen in Fig. 3(b), both theory and experiment show that ε_1 of Ag also vanishes for ≈ 7.7 eV. Since the value of ε_2 is appreciable at this point, this leads to a broad feature in the loss function with the peak position at about 8.0 eV (peak (2) in Fig. 4(b) and Fig. 1(b) of the main paper). Similar to peak (2) of Cu, this peaks is a result of the interplay between the free-electron plasmon resonance, sharp absorption edge from Ag 4*d* bands, as well as higher lying absorption bands. However, due to the vanishing value of ε_1 and the involvement of *sp* electrons, we can attribute this peak also to a plasmon resonance.

Gold. The behavior of the complex dielectric function of Au is rather similar to that of Cu. The position of *d* states is shallower than in Ag, but slightly deeper than in Cu, as seen in Fig. 1(c). Gold appears brownish in GGA (Fig. 5). As before, *GW* corrections of Ref. [10] move the *d* states to slightly lower energies, but these corrections are somewhat less pronounced than in the two previous cases. However, they are sufficient to restore the golden color (Fig. 5). Both theory and experiment show that ε_1 does not become zero for

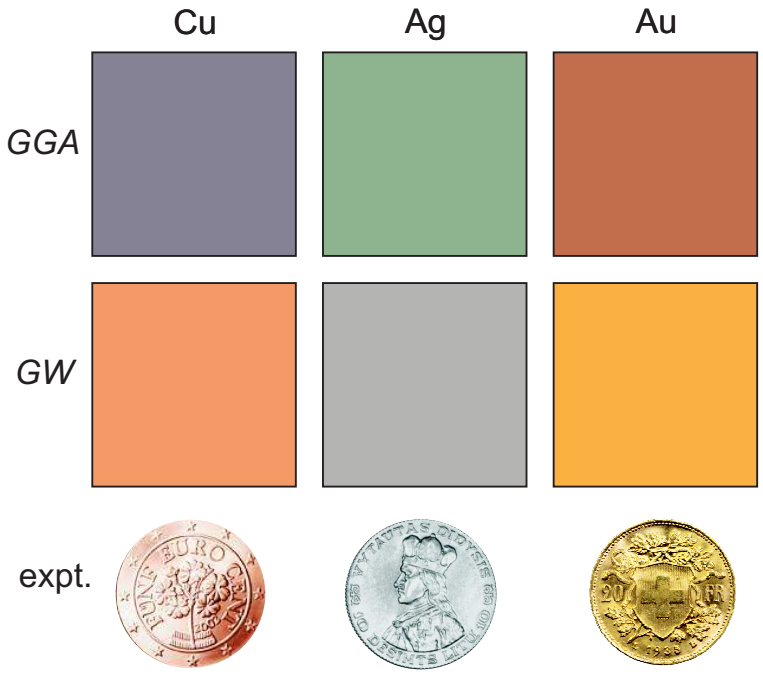

FIG. 5: (Color online) Simulated colors of Cu, Ag, and Au using GGA (top) or *GW* (bottom) band structures. Reflection was modeled by diffuse scattering using the dielectric function calculated within the respective theory. The CIE 1931 XYZ scheme was used to model the resulting colors. The Austrian 5 Euro-cent coin (2006, copper-coated steel), the Lithuanian 10 litas coin (1936, 0.75 fineness silver), and the Swiss 20 franc Goldvreneli (1935, 90% gold) are shown for comparison. The color of real metals results from a combination of diffuse and specular scattering. The latter is responsible for the metallic glare.

energies below 5 eV, but, at variance, it attains small negative values right before the onset of optical transitions from 5*d* states. As a result, a very weak plasmon-like peak (first hump in Fig. 4(c)) develops at 2.65 eV, compared to the experimental value of 2.5 eV. In fact, in the energy range 5.5-6.0 eV, ε_2 is fairly large and ε_1 vanishes due to the interplay of free electrons in the *sp* band, a strong optical absorption band from *d* states to empty states above the Fermi level, as well as higher-lying optical absorption bands. As a consequence, a broad peak in the loss function forms at this energy, which can be also classified as a plasmon-type resonance.

II. INTERBAND TRANSITIONS IN MODEL DIELECTRIC FUNCTIONS

Interband transitions can be described by a set of damped harmonic Drude-Lindhard oscillators with positive frequencies ω_j and damping coefficients γ_j. The corresponding dielectric function is given by:

$$\varepsilon(\omega) = 1 + \sum_j \frac{\alpha_j^2}{\omega_j^2 - \omega^2 - i\omega\gamma_j}, \tag{2}$$

where $\alpha_j^2 = \omega_{\rm p}^2 f_j$, and f_j is the oscillator strength. Let us assume that the frequencies ω_j are well separated from each other, and that the coefficients γ_j are small. In the vicinity of a specific frequency ω_k we can then express the dielectric function as:

$$\varepsilon(\omega) = \beta + \frac{\alpha_k^2}{\omega_k^2 - \omega^2 - i\omega\gamma_k}, \tag{3}$$

where β is the contribution from all other oscillators:

$$\beta \approx 1 + \sum_{j\neq k} \frac{\alpha_j^2}{\omega_j^2 - \omega_k^2}. \tag{4}$$

The loss function around ω_k is given by:

$$L(\omega) = \mathrm{Im}\{-\varepsilon^{-1}(\omega)\} = \frac{1}{\beta^2} \frac{\omega\gamma_k\alpha_k^2}{\left(\tilde{\omega}_k^2 - \omega^2\right)^2 + \omega^2\gamma_k^2}, \tag{5}$$

with

$$\tilde{\omega}_k^2 = \omega_k^2 + \frac{\alpha_k^2}{\beta}. \tag{6}$$

By comparing Eq. (5) and the imaginary part of the dielectric function derived from Eq. (3) we can draw the following conclusions: The peak height of the loss function is renormalized by $1/\beta^2$ in comparison with the corresponding peak in ε_2, and β represents the average value of ε_1 around the peak. Furthermore, the peak is shifted to a higher energy labeled $\tilde{\omega}_k$. The distance between $\tilde{\omega}_k$ and ω_k *decreases* with increasing ω_k. These relations have been used in analyzing the results presented in Fig. 2 of the main text.

III. LOCAL-FIELD EFFECTS IN THE RESPONSE FUNCTIONS

Here we discuss, why at small momentum-transfer q, Cu on the one hand, and Ag and Au, on the other hand, exhibit considerable differences with respect to local-field effects.

We focus on the loss function in the energy range up to 60 eV as shown in Fig. 1 of the main article.

At higher energies the dielectric functions of Cu, Ag, and Au are dominated by transitions from occupied d states. For the energy range, where LFEs are important, the final states are high above the Fermi energy. In essence, they are perturbed free electron-like states. One could expect LFEs to be stronger in Cu as its d orbitals are more localized than those of Ag and Au. Paradoxically, however, the opposite is observed in Fig. 1 of the main article, and we can show that they are weaker in copper *because* of its localized d states. Here, we consider only the RPA response functions for simplicity.

For the present analysis it is convenient to introduce the symmetrized density-reponse function, [12] defined as:

$$\tilde{\chi}^0_{\mathbf{G},\mathbf{G}'}(\mathbf{q},\omega) = \sqrt{v(\mathbf{q}+\mathbf{G})}\chi^0_{\mathbf{G},\mathbf{G}'}(\mathbf{q},\omega)\sqrt{v(\mathbf{q}+\mathbf{G}')} \tag{7}$$

Using this notation, the inverse dielectric constant without local field effects is

$$\varepsilon^{-1}(\mathbf{Q},\omega) = \left[1 - \tilde{\chi}^0_{\mathbf{G},\mathbf{G}}(\mathbf{q},\omega)\right]^{-1}, \tag{8}$$

while the corresponding expression including local fields is:

$$\varepsilon^{-1}(\mathbf{Q},\omega) = \left[\left[\mathbf{1} - \tilde{\chi}^0(\mathbf{q},\omega)\right]^{-1}\right]_{\mathbf{G},\mathbf{G}}. \tag{9}$$

Let us focus on very small momentum transfers q within the first Brillouin zone ($\mathbf{G}$=0). Local-field effects become sizeable if the diagonal elements $\tilde{\chi}^0_{\mathbf{G},\mathbf{G}'}$ become significant. If off-diagonal elements were small, one could expand Eq. (9) in terms of them.

The expansion of Eq. (9) in $\tilde{\chi}^0_{\mathbf{G},\mathbf{G}}$, does not contain linear terms, and to the lowest order in $\tilde{\chi}^0_{\mathbf{G},\mathbf{G}}$ the inverse dielectric function is given by

$$[\varepsilon^{-1}]_{00} = \frac{1}{1-\tilde{\chi}^0_{00}} + \frac{1}{(1-\tilde{\chi}^0_{00})^2}\sum_{\mathbf{G}}\frac{\tilde{\chi}^0_{0\mathbf{G}}\tilde{\chi}^0_{\mathbf{G}0}}{1-\tilde{\chi}^0_{\mathbf{G},\mathbf{G}}} + ... \tag{10}$$

(The arguments of the functions have been suppressed.) The first term of the expansion is the inverse dielectric function without local fields, as given in Eq. (8). Even though the expansion is not strictly valid for Ag and Au (since LEFs are not small), we find that the first term in the expansion has the same sign as the exact expression (i.e. it decreases or increases the loss function in the same way), albeit with a significant overshoot. Eq. (10)

can be written in a more elegant form, similar to the one proposed in Ref. [13]:

$$[\varepsilon^{-1}]_{00} = \frac{1}{1-\tilde{\chi}^0_{00}} + \sum_{\mathbf{G}} \frac{F(\mathbf{G})}{1-\tilde{\chi}^0_{\mathbf{G},\mathbf{G}}} + ... \tag{11}$$

with an appropriately defined weight function $F(\mathbf{G})$. The latter illustrates the coupling of different dielectric functions without local fields at momenta $\mathbf{q}+\mathbf{G}$ to yield the full dielectric function for momentum $\mathbf{q}$.

Actual calculations reveal that the $\mathbf{G}$ vectors within the first shell of reciprocal vectors largely dominate the sum in Eq. (11). We find that the absolute values of the weight function $F(\mathbf{G})$ are by an order of magnitude larger for Ag and Au than for Cu. This, in turn, can be traced back to the matrix elements $\tilde{\chi}^0_{\mathbf{G},\mathbf{0}}$ for Ag and Au being 3-4 times larger than those of Cu for the energies studied.

To understand why this happens we first note that for $\mathbf{q} \to 0$ and $\mathbf{G}' = 0$ the second matrix element in Eq. (10) of the main article is proportional to the momentum matrix element in optical transitions that turn out to be rather similar in Cu, Ag, and Au for comparable energies. It is the first matrix element in this equation, which is more crucial for the observed difference between the metals. It can be written (for $\mathbf{q} = 0$) as $B_{nn'\mathbf{k}}(\mathbf{G}) = \sum_{\mathbf{G}''} c^*_{n\mathbf{k}}(\mathbf{G}) c_{n'\mathbf{k}}(\mathbf{G}+\mathbf{G}'')$, where $c_{n\mathbf{k}}$ is the expansion of Bloch wavefunctions in plane waves. The index n refers to occupied states and n' to unoccupied states (due to the orthogonality condition $B_{nn'\mathbf{k}}(0) = 0$). Therefore, the difference between the three metals with respect to the importance of local fields for energies $0-60$ eV boils down to the different magnitudes of coefficients $B_{nn'\mathbf{k}}(\mathbf{G})$, which we now explain.

Fig. 1 shows that the unoccupied states are perturbed free electron-like states. As a result, the plane wave with $G \approx \sqrt{2E}$ a.u. carries most weight for a given energy E. For energy ~ 70 eV above the bottom of the valence band $G \approx 2.3$ a.u. On the other hand, it is well known from plane wave pseudopotential calculations that in order to accurately describe the d states of noble metals one needs plane waves with the norm up to (approximately) $\sim$ 7 a.u. (50 Ry) for Ag and Au, and ~ 9 a.u. (80 Ry) for Cu. $B_{nn'\mathbf{k}}(\mathbf{G})$ introduced above becomes substantial for unoccupied states n' with $\mathbf{G}$ components that probe the electron density of d states. Since the density of Cu $3d$ states is much more localized, unoccupied states n' that probe this density are higher in energy than for Ag and Au. However, for these higher energies the transitions from shallower semi-core states start to overlap with transitions from Cu $3d$ states.

In summary, we have demonstrated that local-field effects in the energy range $0-60$ eV are smaller for Cu than for Ag and Au because the d orbitals of Cu are spatially more localized. They are thus more extended in the reciprocal space, and are probed by unoccupied states at larger energies.

IV. NORMALIZATION OF EXPERIMENTAL SPECTRA

The dynamic structure factor $s(\mathbf{Q},\omega)$ and the loss function $L(\mathbf{Q},\omega)$ defined obey certain sum rules. Let us first consider a systems where only $N_{\rm eff}$ electrons per unit cell Ω_0 contribute to the electronic excitations, and all the other electrons can be assumed to be frozen. In that case, the dynamic structure factor obeys the so-called f-sum rule,[3] which is (in atomic units):

$$\int_0^\infty s(\mathbf{Q},\omega)\omega d\omega = \pi n_{\rm eff} Q^2, \tag{12}$$

where $n_{\rm eff} = N_{\rm eff}/\Omega_0$. The corresponding rule for the loss function is

$$\int_0^\infty L\left(\mathbf{Q},\omega\right)\omega d\omega = 2\pi^2 n_{\rm eff}. \tag{13}$$

The sum rule cannot be straightforwardly applied to the calculated and measured loss functions in the energy range $0-60$ eV discussed in the main body of the paper. While, to a large extent, for these energies $N_{\rm eff} = 11$ electrons contribute to the response functions, the dielectric functions still vary substantially as a function of energy, and excitations from lower-lying p states start to interfere.

To demonstrate that the f-sum rule indeed holds for theoretical loss functions, thus attesting that our theoretical method is robust, in Fig. 6 we plot the loss functions of Ag for momenta $q = 0.026$ Å^{-1} and 2.128 Å^{-1} in (111) direction up to energies of 130 eV. In this energy range, excitations from $4d$, $5s$, as well as $4p$ levels contribute, and thus $N_{\rm eff} = 17$. Computations to obtain loss functions in this large energy range are very demanding. For energies < 90 eV, the loss function for $q = 0.026$ Å^{-1} is larger in absolute magnitude than that for $q = 2.128$ Å^{-1}. However, as expected from Eqs. (12) and (13), the loss function at larger momenta must become larger than that at smaller momentum, and this indeed occurs above 90 eV in Fig. 6. Because of the prefactor ω in the sum rule, high-energy tails become very important. For energies above 100 eV, the loss functions do not show any pronounced features and decay monotonously. For fitting our data, we assumed a power-law decay of

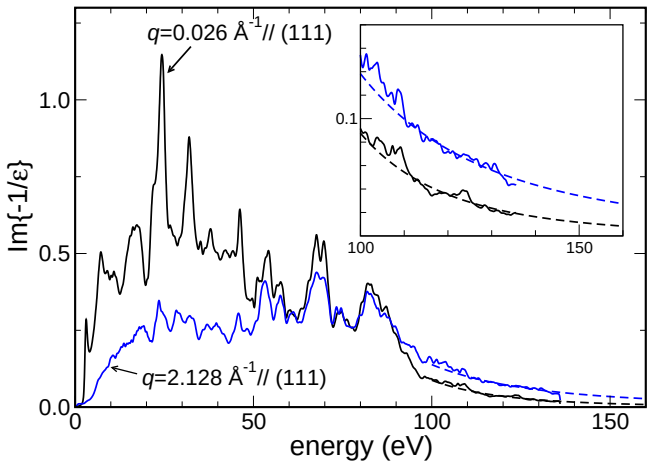

FIG. 6: (Color online) Loss functions for Ag for two different momentum transfers in the energy range $0-160$ eV: $q = 0.026\text{Å}^{-1}$ (black) and $q = 2.128\text{Å}^{-1}$ (blue). The inset shows the high-energy tails of the loss functions that are fitted to the function $A\omega^{\alpha}$.

type A/ω^{α} in the energy range $100-130$ eV. For Ag, the exponent α was very close to 4 for very small Q (inset in Fig. 6), becoming smaller for larger Q (i.e. more extended tail). The sum rule then holds for the loss function defined in this way. For example, it gives $N_{\text{eff}} = 16.81$ and 16.94 for the two momenta in Fig. 6, respectively, thus fulfilling the f-sum rule with an accuracy of 1%. These considerations also show that the decrease of the loss function for larger momenta as seen in Fig. 3 of the main paper is fully consistent with the f-sum rule.

For a vanishing q, an additional sum rule, the so-called screening sum rule, applies: [3]

$$\frac{2}{\pi}\int_0^{\infty} L(\mathbf{Q}=0,\omega)\frac{1}{\omega}d\omega = 1 \tag{14}$$

This sum rule is a consequence of the causality principle, leading to the Kramers-Kroning relationship. The rule is approximately fulfilled for loss functions with a small finite q. For example, it is fulfilled with an accuracy of 0.4% for $q = 0.026$ Å^{-1} shown in Fig. 6.

Both sum rules can be applied to normalize the experimental loss functions. In principle, one could apply the screening sum rule for loss functions at very small momenta. Subsequently, one could calculate N_{eff} from the application of the f-sum rule and scale all other loss functions accordingly. However, the interference of excitations from lower-lying p levels does not allow to apply this procedure. In this work, we have chosen an alternative way where the integral $\int_0^{\omega_0} L(\mathbf{Q},\omega)\, d\omega$ is enforced to have the same value as that based on the

theoretical function. We have chosen $\hbar\omega_0 = 50$ eV.

---

[1] M. A. Cazalilla, J. S. Dolado, A. Rubio, and P. M. Echenique, Phys. Rev. B **61**, 8033 (2000).

[2] C. B. Wilson, Proc. Phys. Soc. LXXVI, 481 (1960).

[3] D. Pines, *Elementary excitations in solids* (W. A. Benjamin, Inc., New York, 1964).

[4] W. Speier, R. Zeller, and J. C. Fuggle, Phys. Rev. B **32**, 3597 (1985).

[5] H. Ehrenreich and H. R. Philipp, Phys. Rev. **128**, 1622 (1962).

[6] A. Otto and E. Petri, Solid State Commun. **20**, 823 (1976).

[7] A. Marini, R. Del Sole, and G. Onida, Phys. Rev. B **66**, 115101 (2002).

[8] A. Marini, PhD thesis, Universitá degli studi di Roma; online at http://www.yambo-code.org.

[9] Z. Yi, Y. Ma, M. Rohlfing, V. M. Silkin, and E. V. Chulkov, Phys. Rev. B **81**, 125125 (2010).

[10] T. Rangel, D. Kecik, P. E. Trevisanutto, G.-M. Rignanese, H. Van Swygenhoven, and V. Olevano, Phys. Rev. B **86**, 125125 (2012).

[11] S. Baroni, *Ab-initio* colors, http://stefano.baroni.me/presentations.html.

[12] M. Rohlfing, P. Krüger, and J. Pollmann, Phys. Rev. B **52**, 1905 (1995).

[13] K. Sturm, W. Schülke, and J. R. Schmitz, Phys. Rev. Lett. **68**, 228 (1992).